

Dependence of slow extraction efficiency from SIS-100 on lattice uncertainties

February 23, 2017

S. Sorge, Accelerator Physics, GSI Darmstadt

Contents

1	OUTLINE	1
2	PREVIOUS WORK	2
2.1	Settings of unperturbed lattice	2
2.2	Magnet imperfections	4
2.3	Beam loss simulations with magnet imperfections: conditions, results, and optimisation	5
3	TEST FOR ROBUSTNESS OF OBTAINED PARTICLE LOSSES	7
3.1	General procedure	7
3.2	Beam Energy $E = 2.7$ GeV/u	8
3.3	Beam Energy $E = 1.5$ GeV/u	9
4	NECESSITY FOR USE OF OCTUPOLES	13
5	Summary	14

1 OUTLINE

In previous studies uncontrolled beam losses during slow extraction from SIS-100 were investigated and estimate by particle tracking simulations. The terminus “previous” in this context refers to work done until and presented at the “Slow Extraction Workshop” which took place in Darmstadt on June, 1-3, 2016. The loss source in these simulations were magnet imperfections added to the unperturbed lattice. Besides estimating the particle losses also optimising the lattice settings in order to minimise particle losses was a major aim of the simulation studies. At that stage only magnet imperfections obtained for highest rigidity were applied because they are the strongest and, hence, the most challenging magnet imperfections. Assuming U^{28+} beams, the highest rigidity $(B\rho)_{max} = 100$ Tm corresponds to the beam energy $E = 2.7$ GeV/u.

The subject of this report is the test for how robust the results obtained in previous studies are against uncertainties in the lattice settings and functions. It

Table 1: Lattice variables of SIS-100 required for slow extraction.

Working point Q_x, Q_y	17.31, 17.45
Horizontal unnormalised chromaticity ξ_x , see Equation (4)	-1
Height of the CO bump at longitudinal ESS position $x_{bu}(s_{ESS})$	-6 mm
Phase space angle of separatrix at horizontal ESS position $x'(x_{ESS})$	1.46 mrad

starts with magnet errors for highest rigidity. In the second step, also magnet errors for medium rigidity will be considered. High intensity effects are not subject of any study presented here.

2 PREVIOUS WORK

2.1 Settings of unperturbed lattice

Initial settings for the unperturbed lattice were provided by D. Ondreka for the working point $Q_x = 17.31, Q_y = 17.8$. In order to avoid crossing of resonances by the the space charge tune footprint in case of high current operation the use of a vertical tune < 17.5 was suggested by V. Kornilov. For that reason, the working point $Q_x = 17.31, Q_y = 17.45$ is used in previous and present studies.

The settings of the unperturbed lattice are the settings of the strengths of quadrupole magnets, sextupoles magnets, octupole corrector magnets, and closed orbit correctors near the electro-static septum (ESS). They are chosen in order to set the working point (Q_x, Q_y) , the horizontal chromaticity ξ_x , the height of a closed orbit bump at the longitudinal position of the electro-static septum $x_{bu}(s_{ESS})$, size and orientation of the stable area in horizontal phase space, to ensure that the latter is triangular, and to minimise beta beating generated by normal-conducting quadrupoles in cell 52 which are longer than the superconducting quadrupoles in all other cells and, therefore, break the six-fold symmetry of SIS-100. The target values of the lattice variables are presented in Table 1.

The magnet strengths which define the lattice variables introduced above are shown in Table 2. The definitions of the magnets strengths are given into the following.

- The working point is defined by the focusing strengths k_1 of the quadrupoles. There are two normal-conducting quadrupoles in cell 52 with length $L_{long} = 1.76$ m whereas the quadrupoles in all other cells are superconducting have length $L_{short} = 1.3$ m which slightly breaks symmetry and results in beta beating. To minimise that, focusing strengths of the longer quadrupoles are set in a way that integrated focusing strengths are

$$(k_{1,f}L)_{long} = 1.05 \cdot (k_{1,f}L)_{short} \quad (1)$$

$$(k_{1,d}L)_{long} = 1.033 \cdot (k_{1,d}L)_{short}, \quad (2)$$

where indices f, d refer to focusing and defocusing, respectively.

- Strengths of resonance sextupoles define size and orientation of the trian-

Table 2: Strengths of magnets for slow extraction with the unperturbed lattice. Some values deviate from those defined by D. Ondreka because the vertical tune $Q_y = 17.8$ was used whereas $Q_y = 17.45$ is used for this study. Only values which are not zero are mentioned.

defocusing short quadrupoles:	$k_1 = -0.2017356388 \text{ m}^{-2}$
focusing short quadrupoles:	$k_1 = 0.2015274258 \text{ m}^{-2}$
defocusing long quadrupole:	$k_1 = -0.1539265849 \text{ m}^{-2}$
focusing long quadrupole:	$k_1 = 0.1562982592 \text{ m}^{-2}$
resonance sextupoles, amplitude:	$(k_2L)_a = 0.76 \text{ m}^{-2}$
resonance sextupoles, phase:	$\phi_0 = 152.79997855650723 \text{ deg}$
“horizontal” chromaticity sextupoles:	$(k_2L)_c = -0.4742956583 \text{ m}^{-2}$
steerer S4EKH1:	$\Delta x' = -0.000324909043 \text{ rad}$
steerer S51KH1:	$\Delta x' = -0.0004466392716 \text{ rad}$
steerer S53KH1:	$\Delta x' = -0.000638492101 \text{ rad}$
octupoles cell 4:	$k_3L = 4.9 \text{ m}^{-3}$

gular stable phase space area and are defined by

$$(k_2L)_n = (k_2L)_a \sin \left(2\pi h \frac{n-1}{n_{periods}} + \phi_0 \right), \quad (3)$$

where $h = 2$ is some kind of harmonic number, $(k_2L)_a$ is the amplitude of the sine or just the “sextupole amplitude”, and ϕ_0 is the “sextupole phase”. $n_{periods} = 6$ is the number of periods of SIS-100 and n is the number a sextupole and of the period it is contained. There is only a single resonance sextupole per period.

- The horizontal unnormalised chromaticity ξ_x defined by

$$\Delta Q_x = \xi_x \delta \quad (4)$$

is reduced to

$$\xi_x = -1 \quad (5)$$

by means of the sextupoles in cells 6, 8, A, and C of each period. These sextupoles have the same strength.

- In order to achieve a clean, triangular stable phase space area it turned out to be necessary to power the octupoles in cell 4 of each period.
- Applying the settings given in Equations (1) and Table 2 the separatrix at electro-static septum position is

$$x'(x_{ESS}) = 1.46 \text{ mrad} \quad (6)$$

which is equal to the pitch angle of the electro-static septum blade.

2.2 Magnet imperfections

In the studies this report is based on linear and non-linear imperfections in alignment and field of dipole and quadrupole magnets are applied.

The linear magnet imperfections are entirely random and defined according to Gaussian distributions truncated at 2σ . For this study applied:

- transverse shifts $\Delta x, \Delta y$ of quadrupoles leading to closed orbit distortion with

$$\sigma_{\Delta x} = \sigma_{\Delta y} = 1 \text{ mm.} \quad (7)$$

- rotations around z axis (tilt) $\Delta\psi$ of the dipoles with

$$\sigma_{\Delta\psi} = 4.04 \text{ mrad} \quad (8)$$

leading mainly to distortion of the vertical closed orbit. $\sigma_{\Delta\psi}$ arises from the assumption that left and right sides of the dipoles are shifted independently according to Gaussian with $\sigma_{\Delta y} = 1 \text{ mm}$, and a full magnet width $w = 0.35 \text{ m}$. $\sigma_{\Delta\psi}$ follows from the double integral

$$\sigma_{\Delta\psi}^2 = \int_{-\infty}^{\infty} d(\Delta y_1) g(\Delta y_1) \int_{-\infty}^{\infty} d(\Delta y_2) g(\Delta y_2) \Delta\psi^2(\Delta y_1, \Delta y_2) \quad (9)$$

with

$$\Delta\psi(\Delta y_1, \Delta y_2) = \frac{\Delta y_1 - \Delta y_2}{w} \quad (10)$$

and

$$g(z) = \frac{1}{\sqrt{2\pi}\sigma_z} e^{-\frac{z^2}{2\sigma_z^2}}. \quad (11)$$

- Deviations in the focusing strengths of the quadrupoles $k_1 L$ with

$$\frac{\sigma_{k_1 L}}{|k_1 L|} = 6.0 \cdot 10^{-4} \text{ (6 units)} \quad (12)$$

resulting in beta beating.

- Deviations in the deflection angle of the main bending magnets α_b with

$$\frac{\sigma_{\Delta\alpha_b}}{\alpha_b} = 4.0 \cdot 10^{-3} \quad (13)$$

resulting in the deformation of the horizontal closed orbit.

It turned out that the closed orbit distortion generates an additional contribution to the beta beating because it imposes random quadrupole strengths in the sextupoles by feed down.

The non-linear imperfections are magnetic field imperfections and lead to resonance excitation and decrease of dynamic aperture. They are introduced by the representation of the magnetic field as series

$$B_y + iB_x = B\rho \sum_{n=0}^{\infty} (k_n + ij_n) \frac{(x + iy)^n}{n!} \quad (14)$$

Table 3: Strengths of magnets for slow extraction with systematic non-linear magnet imperfections for a U^{28+} beam at $E = 2.7$ GeV/u.

defocusing short quadrupoles:	$k_1 = -0.2018027483 \text{ m}^{-2}$
focusing short quadrupoles:	$k_1 = 0.2016372255 \text{ m}^{-2}$
defocusing long quadrupole:	$k_1 = -0.1490588482 \text{ m}^{-2}$
focusing long quadrupole:	$k_1 = 0.148936587 \text{ m}^{-2}$
resonance sextupoles, amplitude:	$(k_2L)_a = 0.45 \text{ m}^{-2}$
resonance sextupoles, phase:	$\phi_0 = 167.799976890095 \text{ deg}$
“horizontal” chromaticity sextupoles:	$(k_2L)_c = -0.6271758065 \text{ m}^{-2}$
steerer S4EKH1:	$\Delta x' = -0.0003428661584 \text{ rad}$
steerer S51KH1:	$\Delta x' = -0.0003212843055 \text{ rad}$
steerer S53KH1:	$\Delta x' = -0.0005074467319 \text{ rad}$
octupoles cell 4:	$k_3L = 0$

with the normal and skew multipole coefficients of order n

$$k_n = \frac{1}{B\rho} \frac{\partial^n B_y}{\partial x^n} \quad \text{and} \quad j_n = \frac{1}{B\rho} \frac{\partial^n B_x}{\partial x^n}. \quad (15)$$

Separate multipole coefficients are applied to the entrance, centre, and exit regions of dipoles and quadrupoles. Each multipole coefficient consists of systematic contribution due to magnet design and random component which arises from random deviations of magnet from design,

$$(k_nL, j_nL) = (k_nL, j_nL)_{\text{sys}} + (k_nL, j_nL)_{\text{rand}}, \quad (16)$$

where random contributions chosen according to Gaussian distribution truncated at 2σ .

For the quadrupole field imperfections multipoles from simulations up to order 15 in the magnet centres and up to order 20 in the magnet ends are used. The rms random components of normal and skew multipole coefficients are 30 % of corresponding systematic normal coefficient, i.e.

$$\sigma_{k_nL} = \sigma_{j_nL} = 0.3 \cdot |(k_nL)_{\text{sys}}|. \quad (17)$$

The systematic multipole coefficients used for describing the imperfections of the dipole fields are obtained from measurements of fields of 2nd FoS dipole, where the strongest imperfections are those for highest rigidity. The rms random components are chosen according to table received from magnet department.

2.3 Beam loss simulations with magnet imperfections: conditions, results, and optimisation

The previous simulations were done for conditions of maximum rigidity and beam energy in order to apply the strongest non-linear field errors. That means $B\rho = 100$ Tm which corresponds to the U^{28+} ion beam energy $E = 2.7$ GeV/u. It turned out that the insertion of magnet imperfections changes the working point,

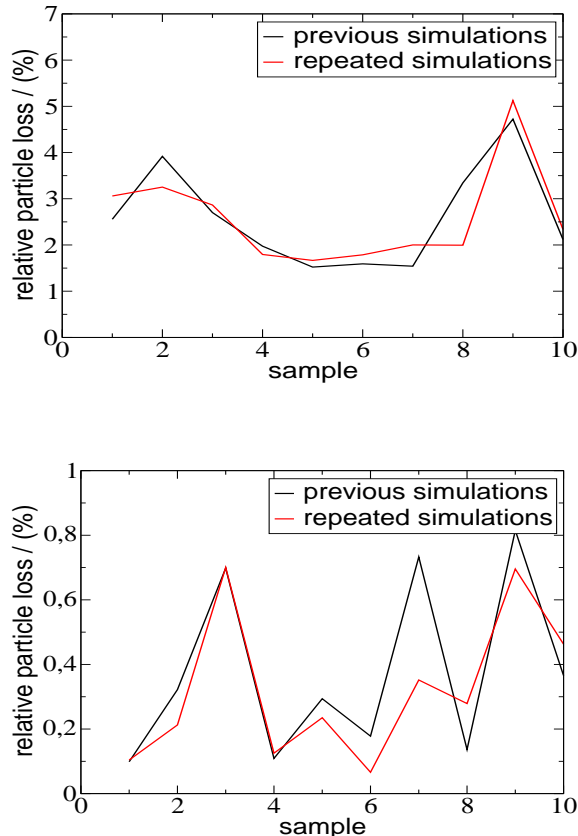


Figure 1: Relative particle loss as function of sample of random errors at the electro-static septum (graph above) and in the ring (graph below) done for the Slow Extraction Workshop (previous) and for this study (repeated). The beam energy is $E = 2.7$ GeV/u.

the horizontal chromaticity, the height of the closed orbit bump at the electro-static septum position, as well as size and orientation of the triangular stable phase space area. To restore working point, horizontal chromaticity, and CO bump height the matching routine is applied for each sample of random errors. New settings for the resonance sextupoles in Equation (3) which define size and orientation of the stable phase space area were found within trial-and-error procedure using single particle tracking. The amplitude of the sextupole strengths, $(k_2L)_a$ in Equation (3) is chosen to be the same for all samples of random errors. Contrary, the phase ϕ_0 in Equation (3) is determined for each sample of random errors individually. That is necessary because ϕ_0 strongly influences the phase space angle of the separatrix at the position of the electro-static septum, $x'(x_{ESS})$, and, hence, the amount of particles lost at the septum. There are major changes of the magnet settings necessary due to the application of magnet imperfections which one can see by comparing Tables 2 and 3. The changes are

- the need for stronger chromaticity correctors because the field of the dipoles has a strong sextupole component. The sextupole systematic coefficients are

$$\text{entrance: } (k_2L)_{syst} = 0.30 \cdot 10^{-1} \text{ m}^{-1} \quad (18)$$

$$\text{body: } (k_2L)_{syst} = 0.14 \cdot 10^{-1} \text{ m}^{-1} \quad (19)$$

$$\text{exit: } (k_2L)_{syst} = 0.36 \cdot 10^{-1} \text{ m}^{-1}, \quad (20)$$

see 2nd last row in Table 6. That results in the increased horizontal natural chromaticity

$$\xi_{x,nat} = -26.7, \quad (21)$$

whereas the horizontal natural chromaticity of the unperturbed lattice is

$$\xi_{x,nat} = -20.2. \quad (22)$$

For that reason stronger sextupoles for chromaticity correction are necessary, compare Tables 2 and 3. The non-linear magnet errors as well as the stronger chromaticity sextupoles result in a reduced horizontal stable phase space area.

- weaker resonance sextupoles to restore the size of the triangular horizontal phase space area and, so, to compensate the influence of the stronger chromaticity sextupoles. If keeping the resonance sextupoles as strong as chosen without magnet errors the stable phase space area would strongly decreased leading to a larger distance between beam and electro-static septum and increased spiral step which results in fast laving of particles during a turn between two passages of the electro-static septum and, hence, to beam loss anywhere in the ring except at the septum.
- The long, normal-conducting quadrupoles in cell 52 have the same integrated focusing strength as the short, superconducting.
- Octupoles are no longer necessary and are switched off.

Finally, 10000 test particles were tracked for 15000 turns in each simulation. To verify the results, some simulations were repeated with the particle number reduced to 5000 in order to make them comparable to simulations for investigating the robustness of the beam losses obtained. Testing the robustness requires many simulations so that computing time becomes a topic to care on resulting in a reduced test particle number. The simulations resulted in

- an average particle loss at electro-static septum: $P_{loss,ESS} = 2.6 \%$.
- an average particle loss anywhere in the ring except at electro-static septum: $P_{loss,ring} = 0.4 \%$.

The particle losses found for 10000 and 5000 test particles are similar, see Figure 1.

3 TEST FOR ROBUSTNESS OF OBTAINED PARTICLE LOSSES

3.1 General procedure

The particle losses found in the study for the Slow Extraction Workshop are low. They could be achieved by “perfect matching”, i.e. precisely matching the magnet settings with knowing and regarding systematic and random magnet imperfections which will not be possible in a real machine. Hence, a test of

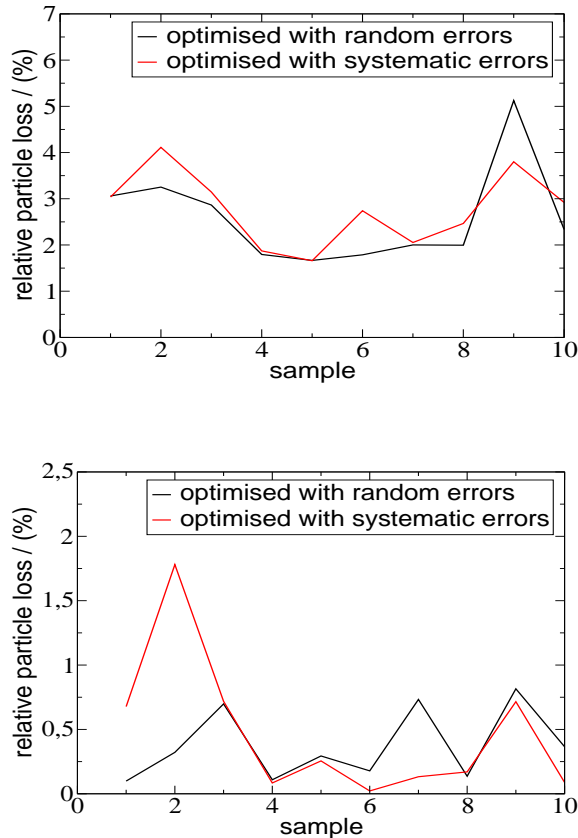


Figure 2: Relative particle loss as function of sample of random errors at the electro-static septum (graph above) and in the ring (graph below) found after matching with all errors and matching only with systematic errors and applying all errors afterwards. The beam energy is $E = 2.7$ GeV/u.

the sensitivity of these beam losses against small lattice changes is started to be performed to estimate robustness of the beam losses.

The test procedure consists of the following step:

1. Define reference lattice and match magnet settings in order to obtain the required machine variables, i.e. working point, horizontal chromaticity, etc.
2. Determine the beam loss with matched reference lattice.
3. Insert perturbations.
4. Determine the beam loss with the perturbed lattice while keeping the magnet settings found for the reference lattice. Compare the beam loss to that found with the reference lattice and to that found with the “perfectly matched” lattice, i.e. which includes and had been matched with all magnet imperfections.

3.2 Beam Energy $E = 2.7$ GeV/u

In the first step the robustness of particle losses for the maximum energy of a U^{28+} beam, $= 2.7$ GeV/u, is investigated because that scenario was considered in the previous beam loss simulations because of the strongest non-linear magnet

imperfections, where the large sextupole error in particular turned out to result in a strongly increased natural horizontal chromaticity, see Equations (21) and (22) or Figure 5. Due to the strong sextupole error strongly modified magnet settings are necessary to enable slow extraction at all. Therefore, the lattice with magnet imperfections differs that strongly from the unperturbed lattice that the latter is no longer a proper choice for the reference lattice. On the other hand, the random variations of the imperfections between the magnets are basically unknown, whereas it should be possible to determine the systematic errors rather precisely. Hence, the lattice only with systematic magnet imperfections is used as the reference lattice and the random variations of the non-linear errors as well all linear errors are considered as small perturbations.

Matching the magnet settings to the reference lattice, i.e. the lattice with systematic errors, particle tracking with the reference lattice yielded an averaged beam loss

- at electro-static septum: $P_{loss,ESS} = 2.6 \%$
- anywhere in the ring except at electro-static septum:
 $P_{loss,ring} = 0.15 \%$.

With lattice matched with systematic errors and inserting systematic and random errors afterwards, the averaged beam losses

- at electro-static septum: $P_{loss,ESS} = 2.8 \%$
- anywhere in the ring except at electro-static septum:
 $P_{loss,ring} = 0.46 \%$, are a little greater than that obtained after matching with random errors included.

were obtained. The beam losses as function of the samples of random magnet errors and initial test particle coordinates are shown in Figure 2.

3.3 Beam Energy $E = 1.5 \text{ GeV/u}$

At the energy $E = 1.5 \text{ GeV/u}$ for a U^{28+} beam corresponding to $B\rho = 62 \text{ Tm}$ the use of magnet settings similar to the original presented in Table 2 turned out to be possible again. The reason is that the systematic sextupole errors in the dipoles are much less than those at maximum rigidity,

$$\text{entrance: } (k_2L)_{\text{sys}} = 0.14 \cdot 10^{-1} \text{ m}^{-1} \quad (23)$$

$$\text{body: } (k_2L)_{\text{sys}} = -0.86 \cdot 10^{-3} \text{ m}^{-1} \quad (24)$$

$$\text{exit: } (k_2L)_{\text{sys}} = 0.15 \cdot 10^{-1} \text{ m}^{-1}, \quad (25)$$

see 6th row in Table 6. Hence, the horizontal stable phase space area remains sufficiently large for providing efficient slow extraction if resonance sextupoles of strength close to original value $(k_2L)_a = 0.76 \text{ m}^{-1}$ are applied. The corresponding magnet settings are presented in Table 4. Remarkable is that no octupole need to be switched on to generate a sufficiently triangular stable area in horizontal phase space.

Matching the reference lattice and using it in the beam loss simulations, the relative beam losses

Table 4: Strengths of magnets for slow extraction with systematic non-linear magnet imperfections for a U^{28+} beam at $E = 1.5$ GeV/u. The amplitude of the resonance sextupoles is $(k_2L)_a = 0.76$ m $^{-2}$.

defocusing short quadrupoles:	$k_1 = -0.2017356388$ m $^{-2}$
focusing short quadrupoles:	$k_1 = 0.2015274258$ m $^{-2}$
defocusing long quadrupole:	$k_1 = -0.1539265849$ m $^{-2}$
focusing long quadrupole:	$k_1 = 0.1562982592$ m $^{-2}$
resonance sextupoles, amplitude:	$(k_2L)_a = 0.76$ m $^{-2}$
resonance sextupoles, phase:	$\phi_0 = 144.67495498907539$ deg
“horizontal” chromaticity sextupoles:	$(k_2L)_c = -0.5324604356$ m $^{-2}$
steerer S4EKH1:	$\Delta x' = -0.000324909043$ rad
steerer S51KH1:	$\Delta x' = -0.0004466392716$ rad
steerer S53KH1:	$\Delta x' = -0.000638492101$ rad
octupoles cell 4:	$k_3L = 0$

- at electro-static septum $P_{loss,ESS} = 5.0$ %
- and anywhere in the ring except at the electro-static septum
 $P_{loss,ring} = 0.66$ %

are obtained. The increase of beam loss at the electro-static septum compared to that found for highest rigidity perhaps arises from the larger vertical beam width.

Matching the reference lattice and applying also random magnet errors in the particle loss simulations yields

- $P_{loss,ESS} = 5.0$ % at the electro-static septum and
- $P_{loss,ring} = 0.31$ % at all other positions in the ring.

Matching the lattice with all errors and using them in the beam loss simulations results in average particle losses

- $P_{loss,ESS} = 4.9$ % at the electro-static septum and
- $P_{loss,ring} = 0.35$ % at all other positions in the ring.

The relative particle losses for the single samples of random errors are shown in Figure 3. The particle losses are obtained to be very similar.

On the other hand, the algorithm for finding ϕ_0 turned out to work not always work properly so that the phase ϕ_0 found for the samples of random errors are not entirely reliable. The reason is that with the magnet errors for medium beam energy the triangular stable phase space area became large enough to almost reach the electro-static septum position so that the determination of $x'(x_{ESS})$ according to the actual ϕ_0 was not unique for the algorithm. Therefore, it seems to be recommendable to choose the resonance sextupoles a little stronger. For that reason resonance sextupole strengths according to

$$(k_2L)_a = 0.78$$
 m $^{-2}$ (26)

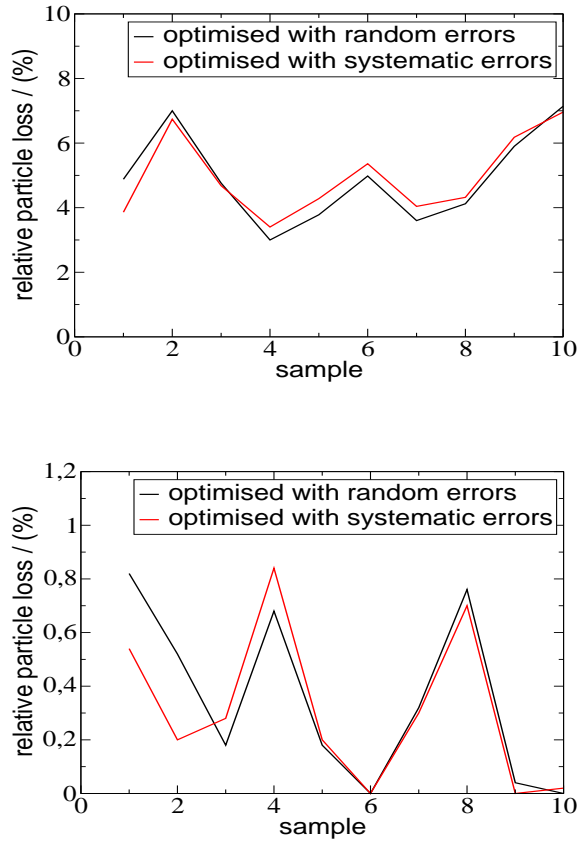


Figure 3: Relative particle loss as function of sample of random errors at the electro-static septum (graph above) and in the ring (graph below) found after matching with all errors and matching only with systematic errors and applying all errors afterwards. The settings applied are those shown in Table 4.

Table 5: Strengths of magnets for slow extraction with systematic non-linear magnet imperfections for a U^{28+} beam at $E = 1.5$ GeV/u. The amplitude of the resonance sextupoles is slightly increased to $(k_2L)_a = 0.78$ m $^{-2}$.

defocusing short quadrupoles:	$k_1 = -0.2017229169$ m $^{-2}$
focusing short quadrupoles:	$k_1 = 0.2015195759$ m $^{-2}$
defocusing long quadrupole:	$k_1 = -0.1539168779$ m $^{-2}$
focusing long quadrupole:	$k_1 = 0.1562921711$ m $^{-2}$
resonance sextupoles, amplitude:	$(k_2L)_a = 0.78$ m $^{-2}$
resonance sextupoles, phase:	$\phi_0 = 145.29997893134714$ deg
“horizontal” chromaticity sextupoles:	$(k_2L)_c = -0.5324426134$ m $^{-2}$
steerer S4EKH1:	$\Delta x' = -0.000324909043$ rad
steerer S51KH1:	$\Delta x' = -0.0004466392716$ rad
steerer S53KH1:	$\Delta x' = -0.000638492101$ rad
octupoles cell 4:	$k_3L = 0$

in the next step, where all other parameters are only changed in order to set the required lattice variables. The magnet strengths set are presented in Table 5. Repeating the simulations for the scenarios as before yields the averaged losses

- $P_{loss,ESS} = 4.5$ % at the electro-static septum and
- $P_{loss,ring} = 0.14$ % at all positions except the electro-static septum,

when using the reference lattice for matching and in the beam loss simulations,

- $P_{loss,ESS} = 4.7$ % at the electro-static septum and
- $P_{loss,ring} = 0.35$ % at all positions except the electro-static septum,

after matching the reference lattice and using systematic and random errors in the beam loss simulations, and

- $P_{loss,ESS} = 5.1$ % at the electro-static septum and
- $P_{loss,ring} = 0.31$ % at all positions except the electro-static septum,

if the lattice is matched with systematic and random errors. The relative particle losses for the single samples of random errors are shown in Figure 4. Regarding systematic and random errors during matching results in particle losses which are slightly higher than those when matching occurred only with systematic errors and all errors were applied in the beam loss simulations. That point is counter-intuitive and should be clarified.

The beam losses obtained with the slightly increased sextupole strengths are in general a little less than those obtained with $(k_2L)_a = 0.76$ m $^{-2}$. Furthermore, the algorithm to find ϕ_0 for each sample of random errors works well because triangular stable phase space area is sufficiently far enough from horizontal position of electro-static septum so that phase space angle of separatrix $x'(x_{ESS})$ can be clearly determined.

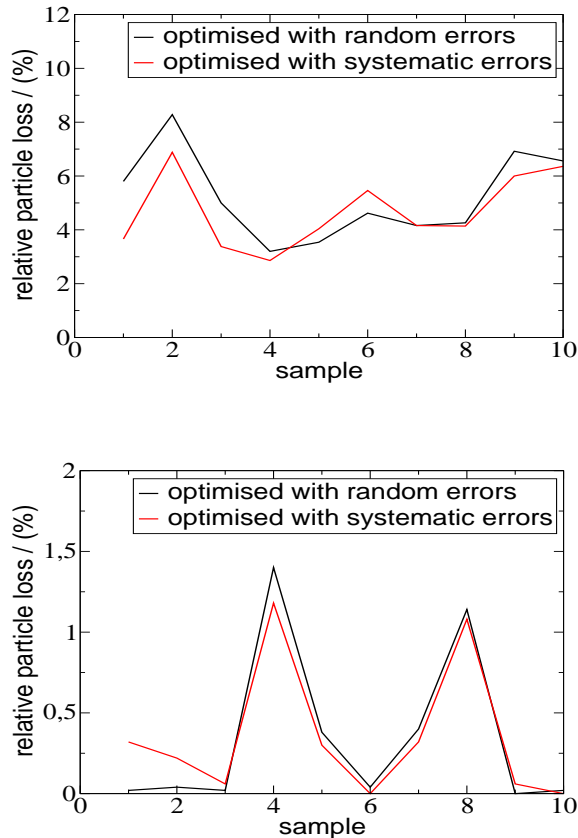


Figure 4: Relative particle loss as function of sample of random errors at the electro-static septum (graph above) and in the ring (graph below) found after matching with all errors and matching only with systematic errors and applying all errors afterwards. The settings applied are those shown in Table 5.

4 NECESSITY FOR USE OF OCTUPOLES

Part of the original settings generated for the unperturbed lattice was the use of octupole correctors which turned out to be necessary for the formation of stable phase space area of clean triangular shape. Instead, when inserting non-linear magnet errors the use of octupole correctors was not necessary anymore. The simplest explanation is that the sextupole errors change the horizontal chromaticity in a way that the influence of the octupoles to correct for some higher order chromatic effects is no longer necessary. From that arises the question whether is that assumption reasonable? To find a comprehensive answer to this question would require the general determination of the higher order chromatic effects which would go beyond the present study. Instead, some single particle tracking simulation are performed for an example to find some threshold for the necessary strength of the sextupole errors and, so, to check whether there is a threshold and to proof the phenomenon to be not a numerical artefact. The latter should be assumed if a triangular stable phase space area could be found for finite but arbitrarily small sextupole errors.

In the example the lattice contains only systematic sextupole errors in the dipoles, where those which correspond to $E = 1.5 \text{ GeV/u}$ or $B\rho = 62 \text{ Tm}$ are applied, see 6th row of Table 6. To find a lower limit, they are consecutively multiplied with a factor $\kappa \in [0, 1]$. The frontier between formation of a triangular

Table 6: Systematic sextupole error coefficients k_2L in entrance, centre, and exit region of the magnetic field of the main dipoles as function of the rigidity. The beam energies correspond to those of a U^{28+} beam. The total sextupole strengths in the last column are the sum of those in the three previous columns.

excitation current/[A]	rigidity [Tm]	beam energy [GeV/u]	entrance $k_2L/[m^{-2}]$	centre $k_2L/[m^{-2}]$	exit $k_2L/[m^{-2}]$	total $k_2L/[m^{-2}]$
500	3.89	0.010	0.0103	-0.0275	0.00977	-0.0074
1000	7.76	0.039	0.0126	$-7.05 \cdot 10^{-3}$	0.0128	0.018
1500	11.64	0.086	0.0135	$-2.14 \cdot 10^{-3}$	0.0134	0.025
2000	15.51	0.149	0.0138	$-3.0 \cdot 10^{-4}$	0.0137	0.027
4000	31.02	0.505	0.0140	$3.38 \cdot 10^{-4}$	0.0139	0.028
8000	61.99	1.45	0.0144	$-8.55 \cdot 10^{-4}$	0.0147	0.028
10000	77.40	1.95	0.0163	$-3.64 \cdot 10^{-3}$	0.0173	0.030
12000	92.19	2.45	0.0228	$-3.75 \cdot 10^{-3}$	0.0261	0.045
13200	100.18	2.72	0.0303	0.0139	0.0361	0.080
13500	102.06	2.79	0.0328	0.0201	0.0393	0.092

and a non-triangular stable phase space area is found for

$$\kappa \in [0.5, 0.6], \quad (27)$$

see red and green curves in Figure 6. One can see that red stable phase space area as well as that determined for $\kappa = 0$ has round corners and no particle leaves the triangle. On the other hand, the green stable phase space area as well as that found for $\kappa = 1$ has sharp corners and leaving particles are visible which denote the separatrices one of which is directed towards the electro-static septum.

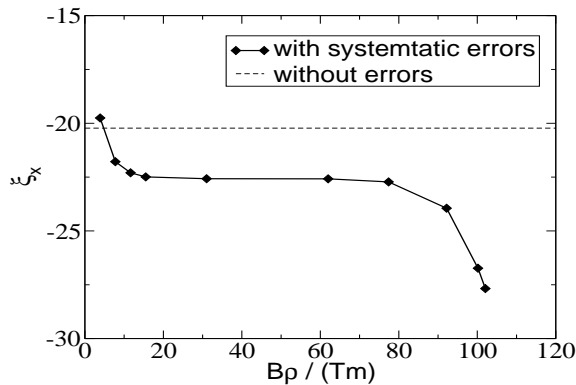


Figure 5: Unnormalised horizontal natural chromaticity of the SIS-100 lattice with systematic magnet imperfections as a function of the rigidity, which corresponds to the excitation current, see Table 6.

5 Summary

Starting from settings for the unperturbed SIS-100 lattice provided by D. Ondreka, particle losses during slow extraction had been estimated by particle track-

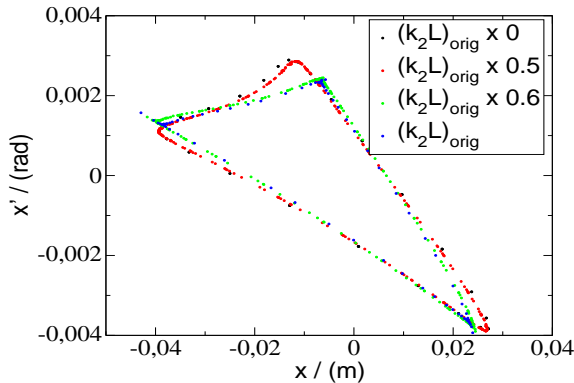


Figure 6: Horizontal stable phase space area determined by single particle tracking for a lattice only with systematic sextupole errors in the dipoles, where $(k_2L)_{orig}$ denotes the sextupole strengths for $B\rho = 62$ Tm in the 6th row of Table 6.

ing after inserting magnet errors. In the first step, non-linear magnet errors for the highest rigidity was included because they are the strongest and, hence, define the most challenging case. Later, also the influence of non-linear errors for an intermediate rigidity was investigated. In particular the inclusion of the errors for highest rigidity resulted in large beam losses and made comprehensive changes of the settings necessary in order to minimise particle losses. In doing so, losses of about 5 % at the electro-static septum and of about 0.5 % at all other positions could be achieved.

The low particle losses could be achieved by perfectly matching the lattice with all magnet errors considered. The aim of the study presented in this report now is to check the robustness of the small particle losses. The robustness is estimated by determining particle losses with a matched reference lattice and with the lattice with magnet errors added and using the settings for the reference lattice. It turned out, that for highest rigidity the unperturbed lattice can not be used as reference lattice because the necessary changes of the lattice settings due the strong magnet imperfections are that large that adding the magnet imperfections would make extraction basically impossible. Therefore, the lattice with systematic errors is used as reference lattice and only the random error contributions are added. The particle losses found are not far above those found with the perfectly matched lattice. That suggests that rather good results could be found if the lattice is optimised with regarding only systematic magnet imperfections.

There are open points which have to be clarified:

- The particle losses of the simulations for conditions at $E = 1.5$ GeV/u at the electro-static septum are found to be in average slightly higher if all magnet errors were included during matching than those found after matching only the reference lattice with systematic errors but applying all errors in the particle loss simulations. That contradicts with intuition because regarding for all magnet errors should yield a better adaptation of the separatrix to the pitch angle of the electro-static and, hence, lower particle loss there.
- The particle losses at the electro-static septum found for intermediate energy, $E = 1.5$ GeV/u, are higher than those found for the maximum energy $E = 2.7$ GeV/u. A possible reason could be that for lower energy the

vertical beam width is greater which increases beam loss. First results of simulations with vanishing vertical beam width, i.e. $\epsilon_{y,beam} = 0$, contradict this assumption because the beam losses found are not less than those found with finite vertical beam width derived from the beam emittance at injection energy and the adiabatic damping according to the extraction energy.

For these points the present report represents a preliminary status and will be extended when there will be new results.